

# A Platform for Autonomous Navigation in Kiwifruit Orchards

Mark H. Jones<sup>a,\*</sup>, Jamie Bell<sup>b,\*\*</sup>, Matthew Seabright<sup>a</sup>, Alistair Scarfe<sup>c</sup>, Mike Duke<sup>a</sup>, Bruce MacDonald<sup>b</sup>

<sup>a</sup>*School of Engineering, University of Waikato, Hamilton, New Zealand*

<sup>b</sup>*Faculty of Engineering, University of Auckland, Auckland, New Zealand*

<sup>c</sup>*Robotics Plus Ltd, Neunham Innovation Park, Tauranga, New Zealand*

---

## Abstract

Systems for performing autonomous horticultural tasks usually require a means of locomotion through their environment. One approach is to directly integrate a drive system at the expense of increasing overall complexity and development risk. We present a generalised mobile platform designed to carry task specific robots through pergola style kiwifruit orchards. The platform is general in the sense that it itself does not perform tasks. It is intended solely to navigate through orchards and be capable of carrying robotic modules.

The selection of sensors best suited for autonomous navigation in this environment is discussed and presented with in-orchard test results. Details of the platform's software and hardware architecture are also discussed. The series-hybrid platform presented here has reliably self-navigated through two test orchards unassisted and is capable of carrying a 1000 kg payload.

### *Keywords:*

Agricultural automation, autonomous navigation, orchard robotics, sensor selection

---

## **1. Introduction**

- 2 Short-term labor requirements within New Zealand's kiwifruit industry  
3 peak twice a year corresponding with the pollination and harvesting of ki-  
4 wifruit. The majority of employment during these peaks is filled by seasonal

---

\*MarkHedleyJones@gmail.com

\*\*jamie977@gmail.com

5 or casual workers (Timmins, 2009). As kiwifruit is the country’s largest horticultural export by value (Statistics New Zealand, 2015), effective automation  
6 in this industry will promote economic growth.  
7

8 Previous work on automated kiwifruit harvesting has been demonstrated  
9 (Scarfe, 2012). That work presented a mobile platform with four integrated  
10 robot arms that were capable of harvesting kiwifruit from pergola style or-  
11 chards. The platform presented here is a second generation of that unit. It  
12 increases modularity by separating the platform from the tasks it performs,  
13 namely harvesting and pollination. This paper discusses only the base plat-  
14 form, where details of modules for pollination and harvesting are published  
15 separately (Williams et al., 2018; Seabright et al., 2017).

16 Automation in kiwifruit harvesting and pollination demands computer  
17 control, state-of-the-art manipulators, and advanced vision based detection  
18 systems. These systems are bulky and have specific geometric requirements  
19 dictated by the environment and the tasks they perform. They share the  
20 requirements of transport in and around orchards, electrical power, and air  
21 pressure. However, they differ in the way they move when in the orchard.  
22 Pollinating modules, developed as part of a wider project, move at a well-  
23 known velocity with minimum changes in steering angle. This differs from the  
24 harvesting module, also developed as part of a wider project, that advances a  
25 set distance between stationary harvest cycles. These modules are designed  
26 to work autonomously and therefore the platform they are attached to must  
27 also be autonomous.

28 It has been stated that “since the robot development already includes  
29 a high complexity, the application itself should be of comparably low com-  
30 plexity” (Ruckelshausen et al., 2009). By separating the development of the  
31 platform from other task-specific modules, the risk of a single part becom-  
32 ing overly complex is reduced. The platform presented here simply needs to  
33 navigate autonomously through kiwifruit orchards.

34 The development of autonomous vehicles in agriculture is not new, but  
35 much of the literature relates to manned vehicles converted to drive-by-wire.  
36 This work details the development of a platform built specifically for navi-  
37 gating pergola style kiwifruit orchards. Key requirements for this platform  
38 are to: be capable of carrying a 1000 kg mass, have a high degree of ma-  
39 neuverability, maximise area available to task specific modules, and navigate  
40 autonomously through pergola style kiwifruit orchards for extended periods.



Figure 1: The robot platform driving through a pergola style kiwifruit orchard.

## 41    2. Related Work

### 42    2.1. Purpose-built Autonomous Vehicles in Agriculture

43    The introduction of computers and digital camera technology during the  
44    1980s sparked research into autonomous vehicles for agricultural use (Li et al.,  
45    2009). When publishing details of an autonomous vehicle in 1999, Tillett  
46    et al. cite difficulties dealing with variability in lighting and the environment  
47    as the reason no commercial vehicles were available at the time. Their ve-  
48    hicle combined wheel encoders, a compass, and accelerometers for odometry  
49    information. It also featured a camera based row guidance system. It was ca-  
50    pable of spraying individual plants whilst autonomously driving at  $0.69 \text{ m s}^{-1}$   
51    ( $2.5 \text{ km h}^{-1}$ ).

52    Three years later, two autonomous robots designed for weed mapping  
53    and control were presented (Pedersen et al., 2002; Åstrand & Baerveldt,  
54    2002). These platforms had relatively simple chassis and drive systems as  
55    they were both at a prototype stage. Both featured two-wheel steering and  
56    were designed specifically for field crops. While both were battery powered,  
57    the platform presented by Åstrand & Baerveldt (2002) could also be fitted

58 with a combustion engine. The vehicle presented by Pedersen et al. (2002)  
59 was designed to follow pre-defined GPS based paths through row crops, but  
60 the authors found that this was impractical without a dedicated row guidance  
61 sensor. They proposed a revised design that featured a row guidance sensor, a  
62 revised drive system with four-wheel steering, and a Controller Area Network  
63 (CAN) bus for low-level communication.

64 Two years later, the revised design proposed by Pedersen et al. (2002)  
65 was presented by Bak & Jakobsen (2004). The authors noted that the control  
66 strategy for the four independently controlled wheels was non-trivial. The  
67 GPS receiver on this platform utilised Real Time Kinematic (RTK) correc-  
68 tions from a base station. RTK-GPS is capable of providing positioning with  
69 accuracies of 2 cm.

70 In 2009, details of BoniRob were published by Ruckelshausen et al. (2009).  
71 Similar to the unit presented by Bak & Jakobsen (2004), it featured a gyro-  
72 scope, RTK-GPS for localisation, a CAN bus for communication, and four-  
73 wheel steering. What makes BoniRob particularly interesting is its ability to  
74 alter its track width by actuating the arms to which its wheels were attached.  
75 A 2.8 kW petrol generator could be mounted to the chassis, additional to its  
76 on-board batteries. It was capable of carrying a 150 kg payload in its dedi-  
77 cated module space. Like the robots before it, BoniRob was designed for use  
78 on open field crops. It introduced the use of both single-plane and multi-  
79 layer laser range scanning, known as lidar, for perception and row detection.  
80 During the previous year, some of these authors published details of a much  
81 simpler robot named ‘Weedy’ (Klose et al., 2008), also an open field crop  
82 based sensing platform.

83 Of particular relevance to this work is that of Scarfe et al. on an au-  
84 tonomous kiwifruit picking robot (Scarfe et al., 2009; Scarfe, 2012). That  
85 work involved the creation of a hydraulically driven platform, with two-  
86 wheel steering, to which four fruit harvesting arms were integrated. While  
87 that platform was designed to navigate kiwifruit orchards autonomously, its  
88 ability to do so was not tested due to an outbreak of *Pseudomonas syringae*  
89 *pv. actinidiae* (PSA) that closed access to kiwifruit orchards. The platform  
90 had an internal combustion engine for on-board power generation. Like the  
91 platform presented here, it was designed specifically for use in pergola style  
92 kiwifruit orchards.

93 Most recently, Bawden et al. (2017) present their field crop robot - Ag-  
94 bot II. For traction it uses two driven wheels in a differential drive configura-  
95 tion, with two castor wheels for support. It is battery powered and designed

96 to autonomously return to a shipping container based shelter with a in-built  
97 solar powered charging station. Their platform is comprised of two side mod-  
98 ules bridged by a wide centrepiece that contains instrumentation. These side  
99 modules contain the drive system, whereas the centrepiece is designed to be  
100 specific to the application. The choice of drive system has considerably re-  
101 duced the robot's complexity and weight over other designs, such as those  
102 previously discussed.

103 Blackmore et al. (2007) envisaged significant reductions in production  
104 costs for agricultural robotics by repurposing parts already in use in the  
105 agricultural and automotive industry. While not a physical component, the  
106 CAN bus is one such technology borrowed from these industries. Most of the  
107 reviewed platforms made use of this communication system. Another trend  
108 is that vehicles designed specifically for open field crops favor four-wheeled  
109 over two-wheeled steering, with the exception of the Agbot II. However, this  
110 configuration may be less useful in an orchard environment. Finally, to aid  
111 development, the use of open source simulation tools allowed the creators  
112 of BoniRob to develop and test their mobility system independent from the  
113 physical hardware.

114 *2.2. Sensors for Row Based Navigation in Orchards*

115 Sensor combinations for orchard based row detection mostly fall into three  
116 categories; camera based, lidar based, or a combination of the two. The  
117 following section summarises a review of row detection efforts in orchards  
118 using these techniques.

119 Subramanian et al. (2006) tested both camera and lidar (Sick LMS-200)  
120 based guidance systems in a citrus fruit orchard. Sensors were trialled sepa-  
121 rately on a tractor retrofitted with a drive-by-wire system. Their vehicle was  
122 able to navigate a small and simplified path using both machine vision and  
123 lidar based approaches at speeds of up to  $4.4 \text{ m s}^{-1}$  ( $15 \text{ km h}^{-1}$ ). They found  
124 that lidar proved more accurate until the lidar's data transfer rate became  
125 a limiting factor. The 2D camera based approach was favorable after this  
126 point. They suggest that combining the two systems would give more robust  
127 guidance as well as providing the ability to detect obstacles. No mention  
128 of the ability for the image based approach to cope with varying lighting  
129 conditions is made.

130 Barawid et al. (2007) demonstrate the use of data from a single-plane  
131 lidar (Sick LMS-219) to guide a drive-by-wire tractor through an orchard.

132 Their results show real-time processing of lidar data is sufficient to navigate  
133 an orchard at  $0.36 \text{ m s}^{-1}$  ( $1.3 \text{ km h}^{-1}$ ).

134 In 2011, two groups published work on the generation of centre lines from  
135 camera data taken in orchard rows. He et al. (2011) uses traditional machine  
136 vision, where Torres-Sospedra & Nebot (2011) makes use of neural network  
137 based image processing. Both methods generate valid paths, although He  
138 et al. note that theirs may not be suitable when the environment background  
139 becomes complex. The neural network based approach of Torres-Sospedra  
140 & Nebot (2011) appears to cope better with variations in lighting and row  
141 spacing. Also in 2011, Hansen et al. (2011) showed the use of a single-plane  
142 lidar (Sick LMS-200) for vehicle localisation in an orchard.

143 The work of Scarfe (2012), combined traditional camera based image pro-  
144 cessing techniques with a single-plane lidar (Sick LMS-111). The image based  
145 approach failed to cope with variability in lighting conditions, however the  
146 lidar proved useful for detecting the trunks and posts in kiwifruit orchards.

147 Freitas et al. (2012) focused on the detection of people and bins in the  
148 rows of an apple orchard using lidar (Sick LMS-291), a low-cost inertial mea-  
149 surement unit, and wheel encoders. Their algorithm was capable of detecting  
150 each obstacle class off-line using data captured from a test orchard.

151 Zhang et al. (2014) used a lidar (Hokuyo UTM-30LX) to generate maps of  
152 an apple orchard with the aid of artificial landmarks. They used an actuated  
153 single-plane lidar to generate multi-plane data for use in row and landmark  
154 based sensing. Placing artificial land-marks in orchards was intended to  
155 reduce the effort required to create orchard maps for guidance systems.

156 The following year, many of the same authors from the paper presented  
157 by Zhang et al. (2014) write about their autonomous vehicle (Bergerman  
158 et al., 2015). It describes an electric utility vehicle converted to drive-by-wire  
159 with the addition wheel encoders for odometry and a single-plane lidar (Sick  
160 LMS-111). While not demonstrated detecting obstacles in real-time, their  
161 previous work processing off-line data (Freitas et al., 2012) has potential to  
162 be integrated on their platform with the addition of extra computing power.

163 Most recently, Sharifi & Chen (2015) write about a method to generate  
164 centre-lines from 2D images of orchard rows. Like the work of He et al. (2011),  
165 the technique offers a way to generate paths from a single camera image  
166 without resorting to neural networks. However, their future work focuses  
167 on increasing robustness to variations in lighting conditions, which indicates  
168 issues in this area. They state their system has use in being complementary  
169 to lidar based navigation.

170      The experiences of Scarfe (2012), and others, indicate that a lidar out-  
171      puts data that requires less post-processing to be robust. The use of lidar  
172      has seen two of the reported vehicles navigate autonomously through orchard  
173      environments, which is encouraging. Other reports suggest that traditional  
174      image based processing for navigation fails when the scene becomes complex  
175      or significant variations in lighting occur. Combining cameras with neural  
176      network based processing increases the robustness to environmental complex-  
177      ities, such as light or clutter, at the expense of increased computation.

178      With regards to the use of RTK-GPS in guidance systems, Slaughter  
179      et al. points out the trade-off of requiring an “unobstructed ‘view’ of the sky  
180      from all parts of the field” (Slaughter et al., 2008). A feasibility analysis by  
181      Pedersen et al. (2006) highlighted the use of RTK-GPS systems as a signifi-  
182      cant cost in yearly subscriptions alone. Durrant-Whyte (2005) describe one  
183      failure mode of GPS being multi-path signal propagation caused by nearby  
184      foliage or the geometry of the land itself. While Li et al. (2009) concludes  
185      that either GPS and machine vision, or GPS and lidar will be used together  
186      as a development trend. Based on the high ongoing cost and increased re-  
187      ception requirements, we discount the use of an RTK-GPS system, but still  
188      consider the use of GPS in-orchard.

### 189      **3. Platform Design**

#### 190      *3.1. Vehicle Configuration*

191      Modules designed to be carried by our platform require clearance from the  
192      canopy in addition to the height they occupy themselves. A kiwifruit canopy  
193      typically varies in height from 1.3 m to 1.7 m between orchards. To maximise  
194      the space available to these modules the platform must be low-slung at the  
195      point they attach. Figure 2 illustrates the platform’s design, with module  
196      area allocated between markers ‘G’ and ‘H’ in the side view (top left). The  
197      top surface of the chassis in this region is 360 mm above the ground.

198      The platform’s steering geometry is Ackermann based. Steering angles  
199      are controlled using the front two wheels which are actuated independently  
200      by brushless AC motors (Heinzmann PSM G100). The ability to actuate the  
201      angles individually simplifies the mechanical geometry needed to coordinate  
202      steering, particularly at extreme angles. Both steered wheels have the free-  
203      dom to rotate 330°, artificially limited by mechanical stops. This allows the  
204      vehicle to pivot about the centre of the rear wheels during tight turns. Be-  
205      cause of this, it is able to turn between rows of kiwifruit vines planted as little

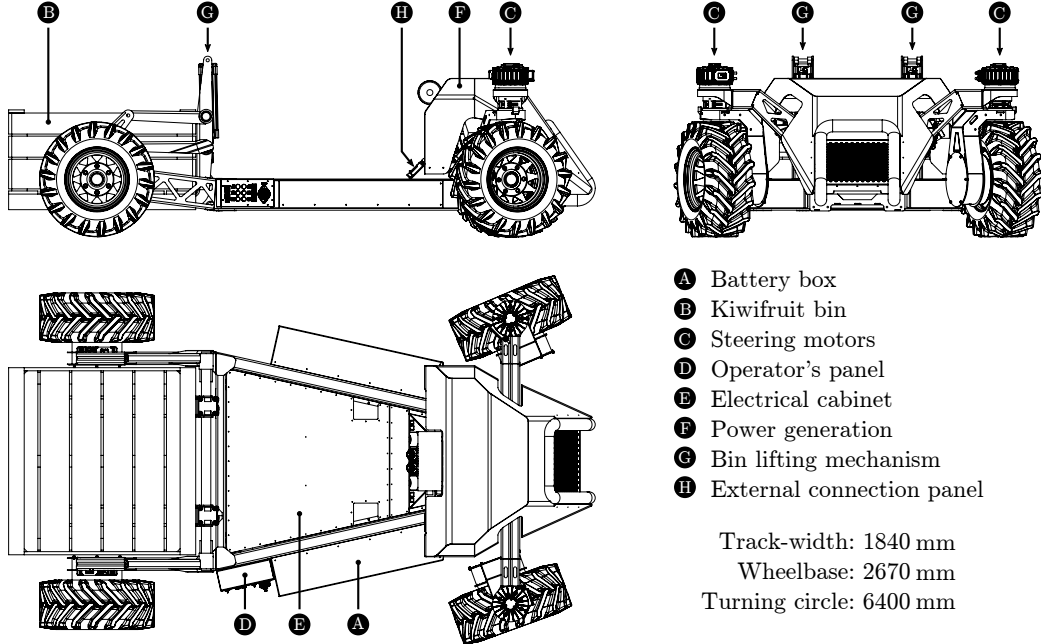


Figure 2: Profile drawings of the robotic platform with kiwifruit bin.

as 3 m apart, satisfying maneuverability requirements. During such a turn, where the centre of rotation is between the rear wheels, the turning circle is equal to twice the vehicle’s length. Implementing four-wheel-steering would shift the pivot point to the vehicle’s centre, roughly halving the turning circle radius. However, headlands in kiwifruit orchards are sized for tractors to turn between rows; tractors with two-wheel steering geometries. Implementing a two wheeled steering system removes the need to develop the “non-trivial” control strategies of a four-wheel steered system and increases the usable platform area. A differential drive, or skid steer, system was expected to cause ground damage to a level considered unacceptable to orchard owners.

Bin lifting forks are fitted to the area between the rear wheels. This area is sized to accommodate a kiwifruit bin. The lifter is actuated by two vertically mounted pneumatic cylinders and is controlled by a standard pneumatic valve block. In future, the platform is expected to have the ability to pick and place bins autonomously while operating in an orchard.

Other than its tires, the platform has no suspension. It features a front pivoting axle which ensures that all four wheels are always in contact with the ground. Each wheel is mounted directly to a 40:1 fixed-ratio planetary

224 gearbox connected to a permanent magnet brushless AC motor (Heinzmann  
225 PSM G120). This specific gearbox-motor combination limits the platform  
226 to a maximum speed of  $10 \text{ km h}^{-1}$ . The lack of suspension is not an issue  
227 when operating in orchards at this speed. In total, the drive system can  
228 continuously deliver 25.6 kW of power and 3.3 kN m of torque. Based on these  
229 specifications it is capable of accelerating from a stand-still to its maximum  
230 speed at an incline of  $20^\circ$  whilst carrying a 600 kg payload in 2.0 s.

231 A power generation unit comprised of a petrol engine (Honda GX-690), air  
232 compressor (Rotorcomp NK-1), and electrical generator (Heinzmann PMSG-  
233 150) sits over the front pivoting axle. The drive shafts of the three units are  
234 connected with a heavy-duty timing belt. The engine, compressor, and alter-  
235 nator can be controlled electronically from an embedded controller module.  
236 This power generation controller module is connected to the rest of the sys-  
237 tem via CAN bus.

238 Fuel and compressed air tanks sit over the right-hand rear wheel, visible in  
239 figure 1. Electrical energy from the power generation unit is fed directly into  
240 the battery modules in a series-hybrid configuration. The fuel tank can hold  
241 approximately 60 l of petrol, allowing the platform to operate continuously  
242 for an estimated period of up to 48 h under light loads.

243 Two battery modules attached to the sides of the chassis each house fifteen  
244 lithium-iron-phosphate ( $\text{LiFePO}_4$ ) batteries connected in series. Together,  
245 the batteries (Winston/Thundersky WB-LYP90AHA) provide a nominal bus  
246 voltage of 96 V and a total electrical capacity of 8.64 kWh. The battery packs  
247 were ‘bottom-balanced’ before being fitted and no cell-level voltage monitor-  
248 ing is present. The maximum and minimum pack voltage was determined  
249 by monitoring individual cell voltages during charge and discharge cycles.  
250 From this battery pack, on-board power supplies can continuously deliver  
251 2.8 kW at 12 VDC, 3.8 kW at 24 VDC, and 3.5 kW at 240 VAC, simultane-  
252 ously, while driving. A connection panel near the front of the platform holds  
253 the weather-sealed plugs through which these outputs are accessible.

254 The chassis was assembled from laser cut and folded steel sections that  
255 were welded together and powder coated. Finite element analysis was used  
256 during its design to help identify areas that required further strengthening.  
257 This helped to ensure the platform met its target carrying capacity of 1000 kg.  
258 This capacity was chosen as the mass of a standard bin of kiwifruit can be  
259 as much as 400 kg, which leaves 600 kg for carrying robotic modules.

260 Unloaded, the machine has an estimated mass of 850 kg, including the  
261 power generation unit and batteries. Testing of the drive system and chassis

262 was performed by driving with a 1000 kg mass strapped to the platform's  
 263 module area. The test included three instances of emergency stopping while  
 264 driving down a 10° slope at a speed of 10 km h<sup>-1</sup>.

265 The battery pack voltage (96 V DC) introduced an electrical hazard that  
 266 required risk mitigation procedures to be followed when working on the unit.  
 267 While essential, these procedures added complexities and delays during de-  
 268 velopment that could have been avoided. The authors suggest a pack voltage  
 269 of 48 V as a safer alternative during development of such vehicles as it bears a  
 270 reduced risk of injury from electric shock. This bus voltage is well supported  
 271 across manufacturers of motors, motor controllers, and power converters.

272 The series hybrid configuration allows the vehicle to drive and provide  
 273 power to subsystems without the petrol engine. This is useful in testing sce-  
 274 narios, where people are in close proximity to the vehicle, as it eliminates  
 275 exhaust fumes and reduces both noise and vibration. However, robotic mod-  
 276 ules and the bin lifting mechanism require pneumatic air pressure to operate.  
 277 As the air compressor is belt driven from the petrol engine, it is necessary  
 278 to frequently run the engine to provide air to these systems. An electric air  
 279 compressor would allow for the system to run without the petrol engine for  
 280 much longer periods. While this is a less energy efficient way of generating  
 281 pneumatic pressure, it would provide a more workable environment during  
 282 testing and development.

283 *3.2. System Architecture*

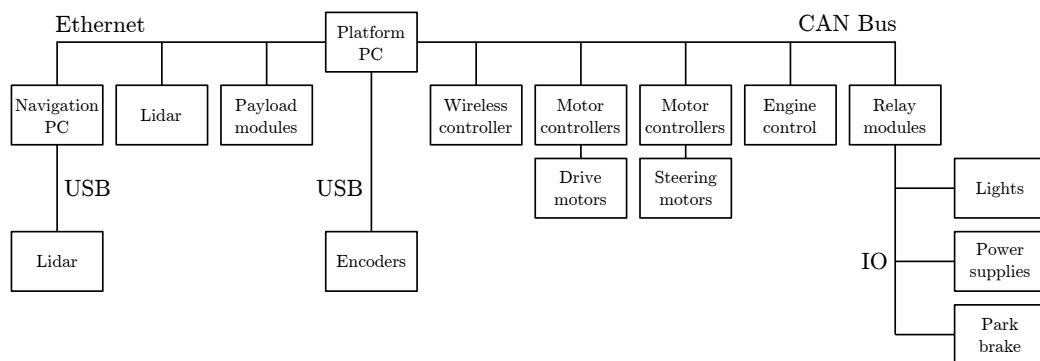


Figure 3: Hardware level system diagram showing the types of interfaces and relative relations on the platform.

284 This section briefly explains the hardware and software architecture of

285 the platform. Standardised protocols and software frameworks are employed  
286 where possible, supplemented with custom solutions where needed.

287 The platform is centrally controlled by an x86 based small-form-factor PC  
288 running Ubuntu 16.04 server. That computer is connected to an on-board  
289 Ethernet network and CAN bus. Low-level sub-systems on the platform such  
290 as motor controllers and relays are connected to this ‘Platform PC’ via CAN  
291 bus. Figure 3 shows a simplified arrangement of connections between each  
292 module.

293 A second computer dedicated to the processing of sensing data for au-  
294 tonomous navigation is connected to the Platform PC via Ethernet. It too is  
295 an x86 based PC running Ubuntu, but uses a microATX form-factor moth-  
296 erboard with a Nvidia GTX 1070 graphics card. This PC is responsible  
297 for computing all aspects of autonomous navigation, such as connecting to  
298 sensors, filtering and processing data, generating drive commands, and com-  
299 municating with the Platform PC. The graphics card is used to accelerate  
300 neural network algorithms and some image processing functions.

301 The open source Robotic Operating System (ROS) is used to facilitate  
302 communication between both computers and between software nodes within  
303 each machine. Figure 4 shows a simplified passage of information entering  
304 through sensors (left hand side), being passed between various nodes, and  
305 finally being fed to the motor controllers. To maximise code reusability, each  
306 device on the platform has its own ROS node dedicated to publishing device  
307 data or subscribing to generated device commands. Interface adapters, motor  
308 controllers, wireless controllers, lidar, and encoders are examples of such  
309 devices. Nodes are also used to transform or perform calculations on data  
310 and pass it between nodes written in either C++ or Python. For instance,  
311 as figure 4 shows, an ‘Ackermann kinematics’ node transforms steering input  
312 data into individual wheel velocity and position/angle outputs. This node  
313 could easily be swapped out for a different translator node during run-time  
314 without disturbing the system.

315 Relay modules allow the Platform PC to toggle power to on-board power  
316 supplies, motor controllers, park-brakes, and lights. These modules also mon-  
317 itor the timing of synchronisation messages transmitted by the Platform PC  
318 onto the CAN bus, which should occur every 20 ms. Once a module de-  
319 tects an absence of synchronisation messages for 100 ms or longer it enters  
320 a defined error state. That state will result in the motor controllers and  
321 on-board power supplies being shut-off and the park brakes engaged. Since  
322 power is required to disengage the park brakes, this equates to ‘shutting-off’

323 the brake release mechanism. CAN bus monitoring ensures that the system  
 324 is automatically shut down should the Platform PC become unresponsive.

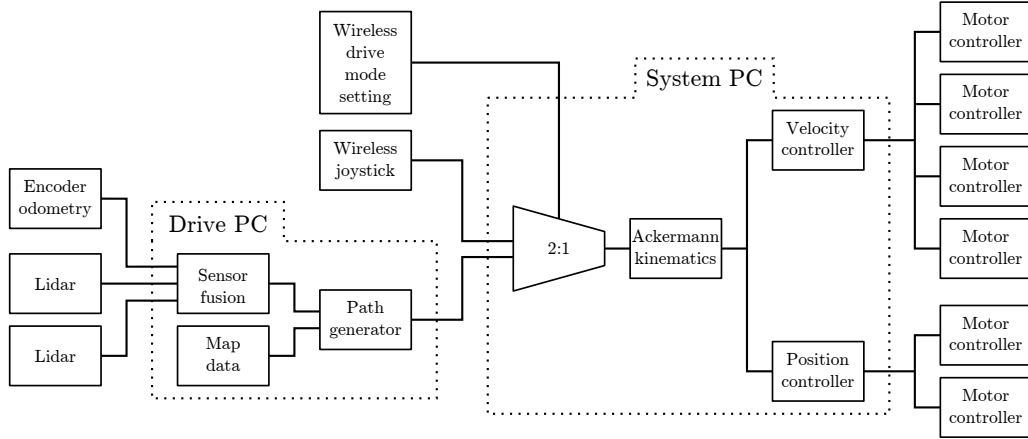


Figure 4: Simplified system diagram (partial) showing node connectivity used for manual and autonomous platform control.

325 In addition to the drive commands generated by the navigation system,  
 326 a safety rated wireless controller (HBC Radiomatic Eco) lets the operator  
 327 issue drive commands via joystick. The joystick also has a mode switch that  
 328 allows the operator to select between manual and autonomous control, and  
 329 an emergency stop button.

#### 330 4. Navigation Sensors

331 The choice of sensors incorporated into a vehicle determines which algo-  
 332 rithmic approaches are available for navigation and object detection. This  
 333 section details the sensor selection and navigation algorithms specific for use  
 334 in kiwifruit orchards. We begin by selecting a number of sensors considered  
 335 appropriate for navigation in this environment. Following this, we test each  
 336 sensor's ability to capture relevant data. Finally, we test the performance  
 337 of appropriate sensors with prototype navigation and object detection algo-  
 338 rithms. An evaluation of each sensor is discussed in the context of orchard  
 339 based navigation.

##### 340 4.1. Sensor Selection

341 As the drive motors have built-in wheel encoders, basic odometry data is  
 342 already available. Encoders on driven wheels will give false readings if wheel

343 slip occurs so should not be used for odometry alone. However, the data  
344 they provide can be used to assist with mapping, localisation, and provide  
345 velocity feedback.

346 Other sensors considered for inclusion are outlined in table 1 with their  
347 associated issues. Factors considered were strengths and weaknesses in the  
348 context of orchard use, reported usage in literature, and availability at a  
349 suitable price. The investigation highlighted both lidar and 2D cameras as  
350 offering high functionality for navigation and object detection. Time-of-flight  
351 cameras were a compelling option based on a cost-benefit analysis; especially  
352 if cheaper units work in sunlight. Because localisation is such a key function,  
the performance of GPS has also been evaluated.

Sensor Type	Possible Issues
GPS receiver	Prone to signal loss from surrounding foliage
Inertial Measurement Unit	Error accumulation and thermal drift
Digital Compass	Prone to disturbance by nearby metallic structures
Encoder	Error accumulation
Lidar	Reduced visibility in fog and heavy rain
Time of Flight Camera	Reduced visibility in sunlight, fog and heavy rain
Camera	Reduced visibility in fog or direct sunlight
Thermal Camera	Reduced visibility in conditions of low thermal contrast

Table 1: Sensor types considered for inclusion on the platform.

353

#### 354 4.1.1. In-orchard GPS Evaluation

355 Two GPS modules were evaluated: a Ublox Neo-M8N module and an  
356 OmniSTAR 5120VBS with AX0 series antenna. Both were connected to  
357 a single board computer (Beaglebone Black) via serial connection for data  
358 acquisition. The Ublox module was selected for its high sensitivity and inter-  
359 internal low-noise amplifier. The OmniSTAR receiver was chosen for its external  
360 high-gain antenna (34 dB) which claims multi-path rejection.

361 The testing procedure first involved planning a path through a single  
362 row of a kiwifruit orchard and plotting this on a satellite map. Waypoints  
363 were placed along the row at the location of posts used to hold the canopy's  
364 structure. Relative distances between these waypoints were measured with a  
365 tape measure and recorded. The receivers were then tested separately over  
366 the course of approximately two hours. Before testing, each unit was powered  
367 up and given 30 min to initialise in an open area near the kiwifruit orchard.  
368 During testing, each unit was walked slowly along the pre-determined path

369 with stops at each waypoint to provide time for a positional fix. The path was  
370 approximately 500 m in length and took approximately 15 min to complete,  
371 including stops at each waypoint. Waypoints were spaced at intervals of  
372 5.5 m along the row.

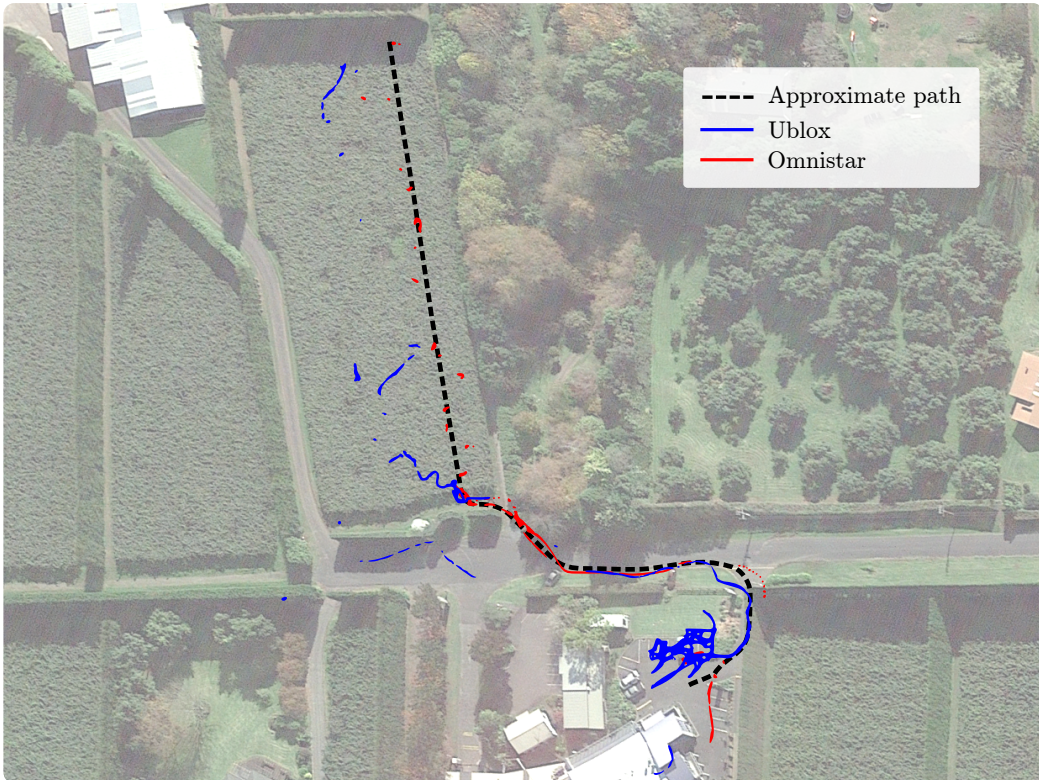


Figure 5: Aerial view of the path taken through the test orchard and the captured GPS data.

373 The path followed, and the corresponding GPS locations collected from  
374 the receivers, is presented in figure 5. It should be noted that data has been  
375 recorded for the round-trip so represents two passes along the path. It was  
376 noticed during testing that the signal quality lights on both GPS receivers  
377 regularly indicated a loss of signal.

378 The Omnistar receiver appears to track the approximate path well, but  
379 the data is sparse with regular loss of signal after entering the orchard. The  
380 Ublox receiver collected more data, but was much less accurate. It may  
381 be possible to use a unit such as the Omnistar, which provided fewer but

382 more accurate readings, as a sanity check for an approximate location within  
383 orchards. Overall, the units could not be relied on for localisation in this  
384 environment. Based on these results we consider GPS receivers similar in  
385 performance to those trialled to be unsuitable for use in kiwifruit orchards.

386 *4.1.2. In-orchard Lidar Evaluation*

387 Three lidar were evaluated, two single-plane and one multi-layer. The two  
388 single-plane lidar were the Hokuyo UTM-30LX and a SICK LMS111. The  
389 multi-layer lidar is a Velodyne VLP-16 which has 16 horizontal 360° planes  
390 spread over 15° vertically. Data was collected from each lidar by driving  
391 through orchard rows with the sensor placed midway between the ground  
392 and canopy (approximately 0.8 m above the ground).

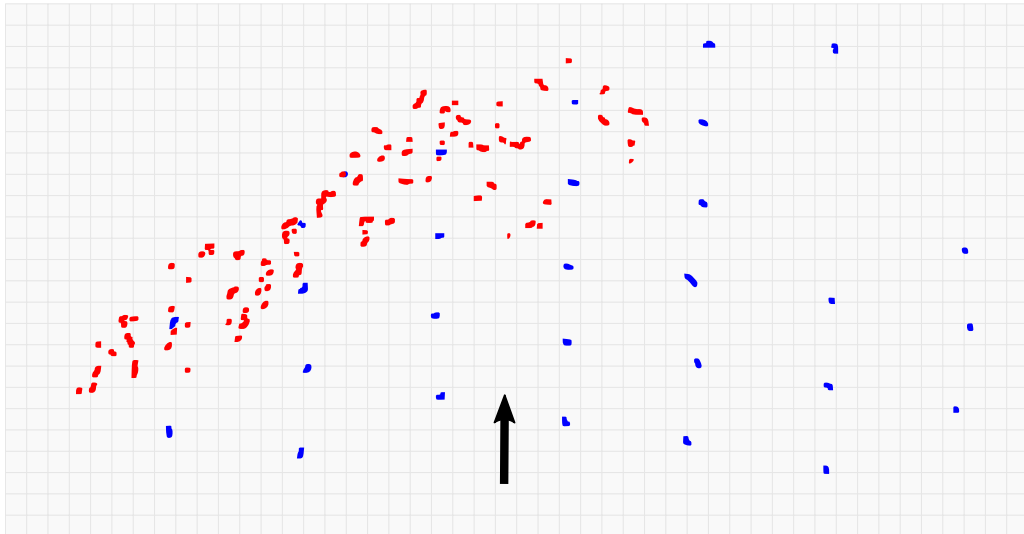


Figure 6: Captured lidar data showing the non-structural points reflected by the canopy (indicated by red markers) and structural points from tree trunks and posts (blue markers). The arrow indicates the position and heading of the platform at the time of capture.

393 The intention was to use lidar as a means of detecting structure defining  
394 features of the orchard, such as posts, trunks and hedges. Detecting these  
395 features should allow for row boundary detection, or general mapping and  
396 localisation. However, both single-plane lidar produced clouds of unstruc-  
397 tured data amongst the structured features, as shown in figure 6. This was  
398 caused by the lidar's scan plane intercepting with the canopy whilst driving

399 over convex terrain. Similarly this issue arose on concave terrain where the  
400 plane intercepted with the ground, as depicted in figure 7.

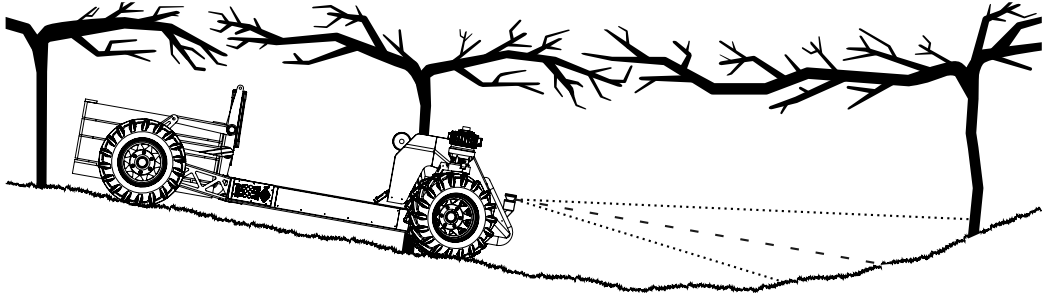


Figure 7: On concave slopes the lidar scan plane intercepts with the ground instead of trunks or posts. The dashed line shows a horizontal plane coming from the the lidar. Dotted lines represent the upper and lower layers taken from the multi-layer lidar.

401 This issue was reduced by the use of a multi-layer lidar and post-processing.  
402 Having sixteen layers available meant it was possible to select a scan layer  
403 that gives the most useful viewing range. Referring to figure 7, that would  
404 correspond to the dotted line above the horizontal (dashed) line which inter-  
405 cepts with a row defining feature (a tree trunk).

406 It was decided that a multi-layer lidar would be best suited for navigation  
407 due to its ability to see more distant features while driving on undulat-  
408 ing ground. A single-plane lidar could still be used at short range as an  
409 independent channel of processing for redundancy or obstacle detection. On  
410 our platform, a single-plane lidar was fitted as a detector for possible colli-  
411 sions, and a multi-layer lidar was fitted for navigation use and general object  
412 detection.

#### 413 *4.1.3. In-orchard Camera Evaluation*

414 Three varieties of camera were tested: time-of-flight, 3D stereoscopic, and  
415 traditional 2D cameras.

416 The time-of-flight based camera was the Basler TOF640-20GM-850NM.  
417 It provides range, intensity, and confidence data at a resolution of 640 by  
418 480 pixels. This specific model was chosen as it had previously proved useful  
419 when collecting depth data of kiwifruit canopies. During that time it had  
420 been operated under different lighting conditions and exhibited minimal oc-  
421 currences of data loss. However, these navigation based tests revealed that in  
422 both direct sunlight and overcast conditions there was significant data loss.

423     The 3D stereo camera tested was an Intel RealSense R200. It combines  
424     a stereo pair of infra-red cameras with a colour camera. Additionally, it  
425     features an infra-red projector as a means of adding texture to objects in its  
426     field of view to assist with stereo processing. The appealing characteristics  
427     of this sensor were its low cost and its claim of being long-range and able to  
428     work outdoors. However, in both overcast and sunny conditions it suffered  
429     from a complete loss of range data.

430     Finally, 2D-cameras were trialled. These were the Basler Dart daA1600-  
431     60uc, Flir CM3-U3-13S2C-CS, and Logitech C920 cameras. Like the lidar  
432     tests, each camera was driven through the orchard at a height of 0.8 m from  
433     the ground. The Logitech C920 suffered from significant motion blur. Being  
434     a consumer grade web-camera this was not surprising; it also lacks a hardware  
435     trigger interface. A hardware trigger becomes important if the camera is used  
436     in stereo vision applications. The Basler and Flir cameras both produced  
437     images of sufficient quality. The Basler offering was favored for its later  
438     model image sensor.

439     Overall, the more industrial 2D camera images (from the Basler and Flir  
440     cameras) were deemed suitable for object detection and classification. This  
441     was verified by processing the data using readily accessible detection algo-  
442     rithms such as convolutional neural networks, which are discussed next. Both  
443     the time-of-flight and 3D stereoscopic camera systems were deemed unsuit-  
444     able based on the occurrences of data loss while operating in direct sunlight  
445     or overcast conditions.

#### 446     *4.2. Sensor Demonstration by Prototype Algorithm*

447     Basic tests indicated that multi-layer lidar and 2D cameras were best  
448     suited for use as primary in-orchard navigation sensors. Further testing with  
449     prototype navigation algorithms ensured that these apparent sensor benefits  
450     translated into practical advantages.

451     The three goals for the navigation system are:

- 452         • object detection and classification,
- 453         • mapping and localisation, and
- 454         • orchard row tracking.

455     To validate that the sensors could perform these functions, three prototype  
456     navigation algorithms have been created.

457 *4.2.1. Object Detection and Classification*

458 Based on existing success using convolutional neural networks for image  
459 processing tasks (LeCun et al., 2015), a camera based system was chosen  
460 for object detection and classification. The network architecture chosen was  
461 FCN-8s (Long et al., 2015). It is a neural network made of convolutional lay-  
462 ers without fully connected layers. FCN-8s performs semantic segmentation,  
463 which refers to the per-pixel classification of images.

464 To train the FCN-8s network, the same image dataset used to assess  
465 camera performance earlier was hand labeled. Labeling involved drawing  
466 object outlines in each image, filling those outlines with colours corresponding  
467 to the object's type, and filling any non-labeled areas with black. Each  
468 image was then converted to an indexed colour file format. An example of  
469 an original image and its corresponding label image is shown as figure 8.

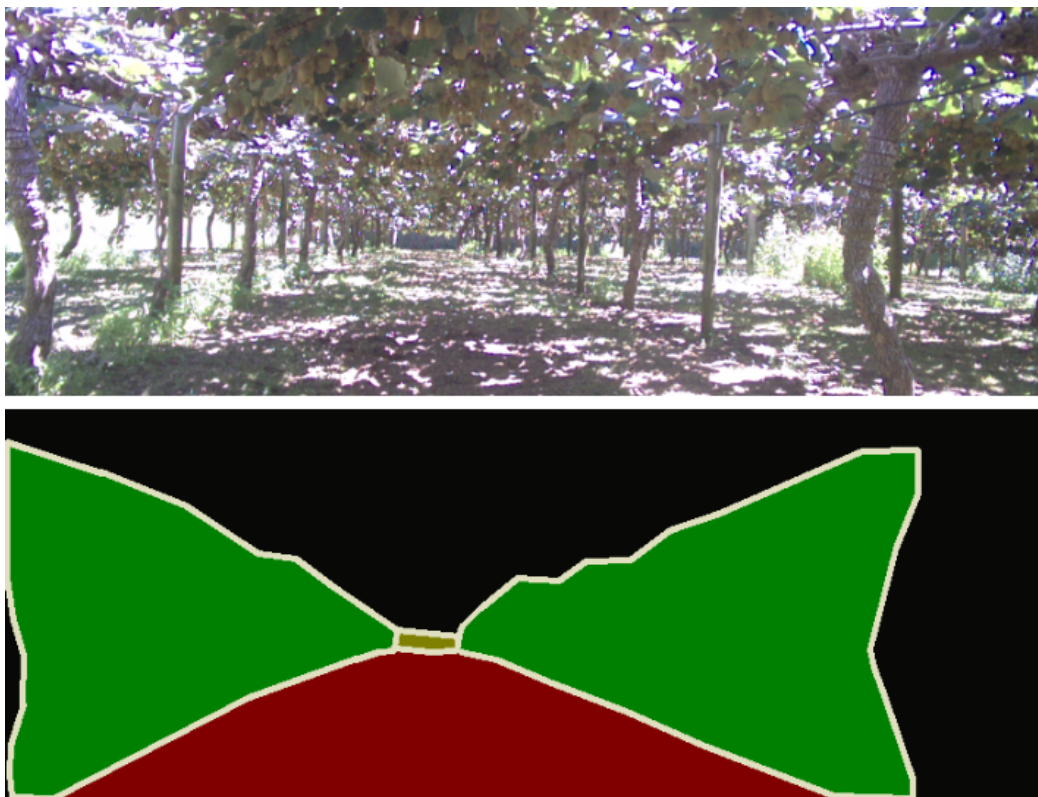


Figure 8: An input image (top) and labeled output (bottom) used to train the semantic segmentation network.



Figure 9: An example inference result from the trained FCN-8s network.

- 470 Initially, individual trees and posts in the kiwifruit orchard were labeled.  
 471 It was later found that labeling the entire tree-line as a single class gave more  
 472 robust results. Objects labeled for this algorithm are:  
 473     1. traversable space (labeled as red),  
 474     2. treelines (labeled as green), and  
 475     3. the end of the current row (labeled as tan).

476 Traversable space was defined as the ground area that the platform could  
 477 drive directly to without collision. These labeled images were then used  
 478 to train the FCN-8s network. Sample output from the trained network is  
 479 presented as figure 9.

#### 480 4.2.2. Mapping and Localisation

481 An existing Simultaneous Localisation And Mapping (SLAM) package  
 482 was used to test the multi-layer lidar. The package used was Gmapping  
 483 (Grisetti et al., 2007), implemented as a ROS package (Gerkey, 2010). Re-  
 484 quired input for Gmapping is odometry data and a single plane of lidar  
 485 data. Odometry information was provided by the platform's in-built wheel  
 486 encoders.

487 As the multi-layer lidar has 16 scanning layers, a conversion was neces-  
 488 sary to produce the single plane of data required by Gmapping. The sim-  
 489 plest conversion from multi-layer data to a single plane would be to select  
 490 one of the available planes and discard the remaining data. However, that  
 491 approach would loose any benefit offered by the multiple scanning layers.

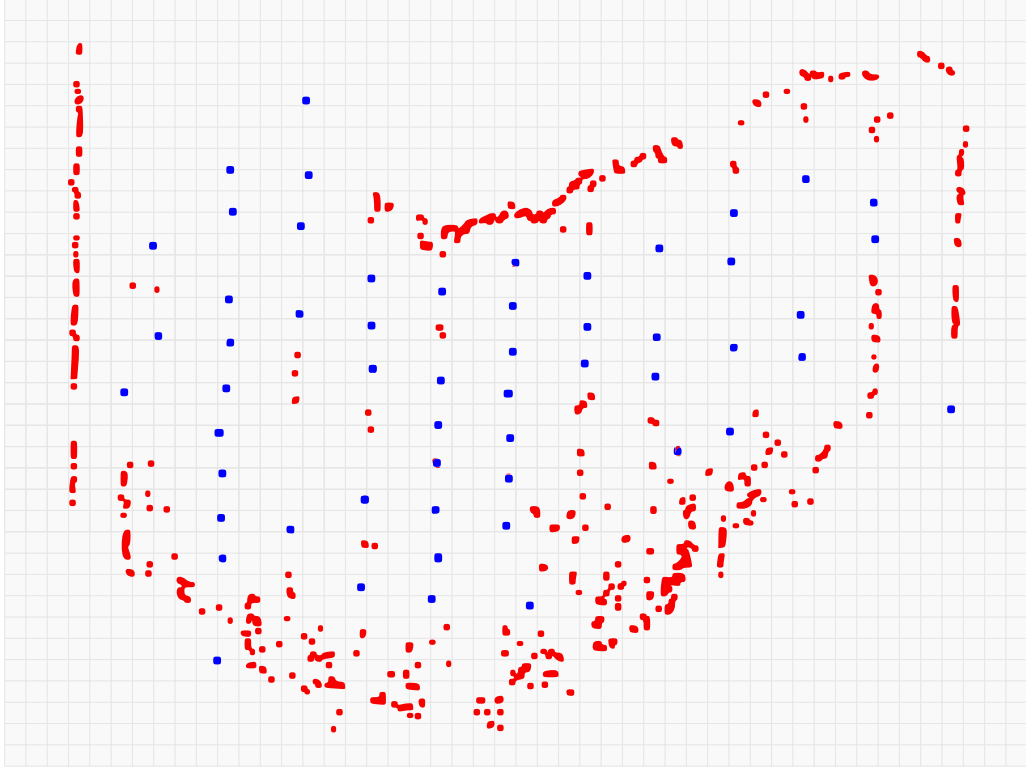


Figure 10: Processing of multi-layer lidar data into a single plane equivalent. Blue points are those selected by the algorithm for further processing, whereas red points are rejected.

Instead, filtering the multi-layer data into a single plane was done by examining the centre four scan layers at each azimuth. With this algorithm, if the range difference between all four points at a single angle falls below a certain threshold, the closest point is returned. Alternatively, if the spread in points is above the threshold, no points are returned. This eliminates points from sloped or varying surfaces while still returning points from objects with vertical structure. The effect of this is that the orchard's structural elements remain visible, but ground and canopy information are removed.

The filtered points are then fed into Gmapping as a single plane with data from the platform's wheel encoders. Figure 10 shows the method's ability to filter structural elements from data containing significant canopy and ground reflections. Using this method, a SLAM based map of the orchard was created and is presented as figure 11.

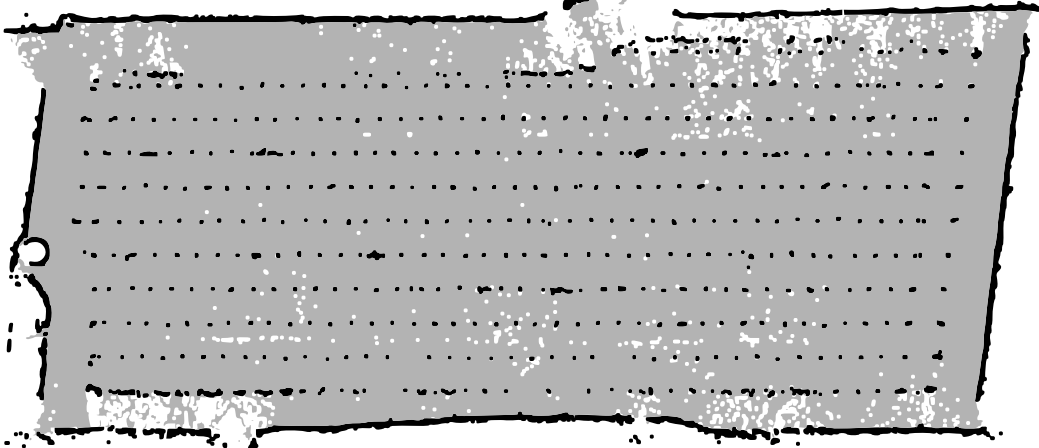


Figure 11: A resulting SLAM based map of a kiwifruit orchard created using Gmapping. Data for the map was collected by traversing four of the orchard’s ten rows. Odometry information has been taken from wheel encoders and a multi-layer lidar (Velodyne VLP-16).

505    *4.2.3. Kiwifruit Orchard Row Tracking*

506    Our final navigation test required interpreting the orchard’s structure for  
 507    the purpose of path generation. For this, a row guidance system was devel-  
 508    oped and tested. It uses the multi-layer to single-plane data filtering tech-  
 509    nique discussed previously. This algorithm also makes use of the platform’s  
 510    on-board wheel encoders. Details of this algorithm have been published sep-  
 511    arately (Bell et al., 2016). The key function of this algorithm is computing  
 512    the angular offset of the platform from the row’s centre-line.

513    A visualisation of data captured whilst navigating the kiwifruit orchard is  
 514    presented as figure 12. The method does not perform SLAM, so the visualised  
 515    data represents only the sensor’s current input, i.e., previous sensor data is  
 516    not considered. Figure 12 shows that while the algorithm is not perfect, it  
 517    does perform reasonably well at identifying orchard structure and generating  
 518    valid headings.

519    *4.3. Sensor Selection Conclusions*

520    The results from prototyped algorithms indicate that the multi-layer lidar  
 521    and wheel encoder feedback are enough for mapping and localisation. This  
 522    combination alone has proven successful for autonomous driving in kiwifruit  
 523    orchards. A combination of 2D cameras and neural networking was suitable  
 524    for object detection and classification. Further research toward using this as

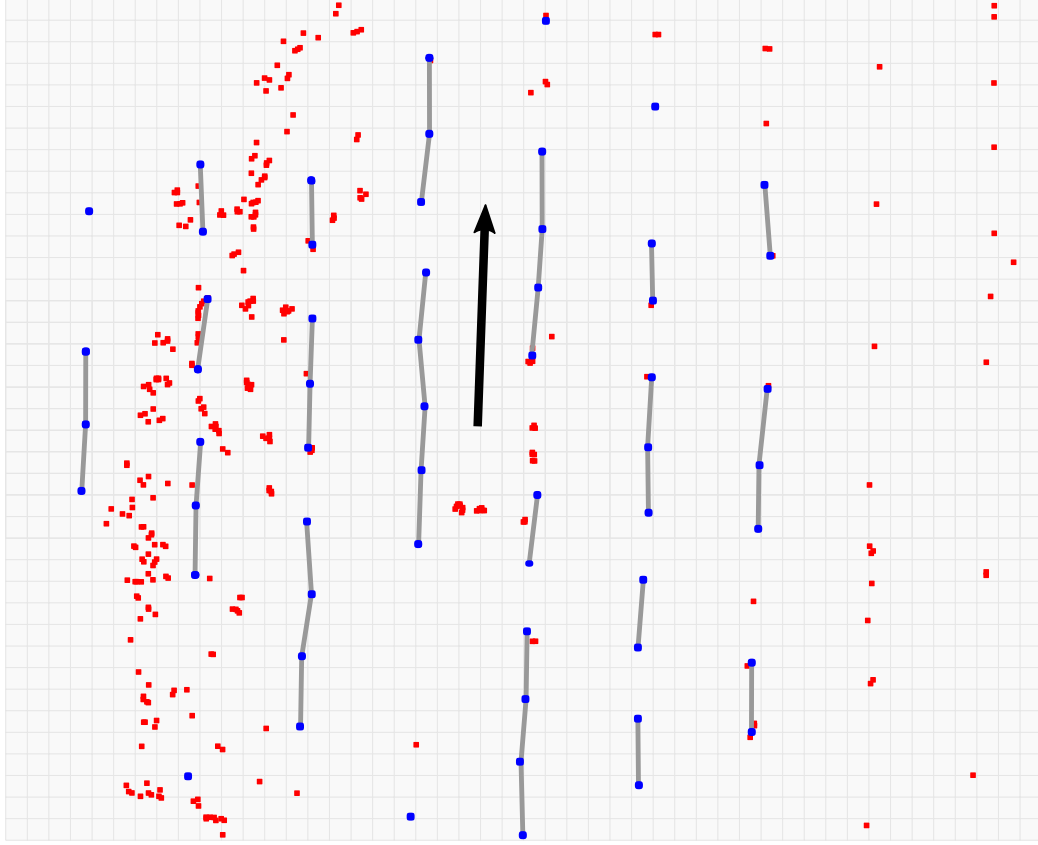


Figure 12: Row detection from multi-plane lidar data. Red points indicate non-structured data that have been ignored. Blue points indicate orchard structure data used for row navigation. Grey lines link orchard structure points by their nearest neighbors (performed algorithmically). The black arrow represents the centreline of the row current row.

525 a means of generating a path for row following is underway and is expected  
 526 to be published in future.

## 527 5. Autonomous Driving

528 Using the row following algorithm developed for sensor testing, map based  
 529 autonomous navigation of a kiwifruit orchard was implemented. Two key  
 530 additions were required for the platform to navigate the orchard unassisted:  
 531 the detection of a row's end and a method for turning between rows.

532 The detection of a row's end is made by detecting a minimum volume of  
 533 free space above the multi-layer lidar. Put simply, this equates to searching

534 for a lack of canopy above the robot. This approach makes use of the multi-  
535 layer lidar, where layers above the horizontal are used as an ‘absence of  
536 canopy’ detector.

537 Turns between rows are performed by driving a series of set curvature  
538 movements while simultaneously performing lidar based obstacle avoidance.  
539 The series of set turns are recorded in a map file which are followed by the  
540 platform at the end of each row. A turn sequence sees the platform drive  
541 with a given steering angle for a given distance or until a given heading is  
542 achieved. Each row turn can contain any number of these sub-maneuvers.  
543 On completion of a turn, row following behavior is resumed which guides the  
544 platform through the row to the next turn. Figure 13 shows the platform  
545 performing a row-end turn while under autonomous control.



Figure 13: Photo of the platform performing a row-end turn in the headland area of a kiwifruit orchard while under autonomous control.

546 Using the approaches developed here, the platform is routinely able to  
547 navigate two test orchards unassisted. Our primary test area is over 1 km in  
548 total traversable length, spread over 10 rows. The developed algorithm has  
549 been used to autonomously control this platform and two smaller platforms  
550 through 20 km of kiwifruit orchards.

551    **6. Conclusion**

552    In this work, a platform designed specifically for driving through pergola  
553    style kiwifruit orchards has been presented. The platform has the capability  
554    of carrying a payload of up to 1000 kg through these orchards with minimal  
555    performance degradation. We identify 48 V as a sensible bus voltage on de-  
556    velopment vehicles such as this. Sensors suitable for autonomous navigation  
557    have been selected, trialled and demonstrated as being useful as a means  
558    of navigating in this environment. Convolutional neural networks applied to  
559    monocular images proved to be a promising technique for row navigation and  
560    further work in this area is under-way. By processing multi-layer lidar data  
561    the platform presented here can reliably navigate an orchard block without  
562    human intervention.

563    **Acknowledgements**

564    This research was supported by the New Zealand Ministry for Business,  
565    Innovation and Employment (MBIE) on contract UOAX1414. The authors  
566    acknowledge contributions from Phillip Ross, Gordon Neshausen, Josh Bar-  
567    nett, and Erin Simms who were involved with the design and fabrication of  
568    the platform, and assistance testing and training neural networks from Nicky  
569    Penhall.

570    **References**

- 571    Åstrand, B., & Baerveldt, A. J. (2002). An agricultural mobile robot with  
572    vision-based perception for mechanical weed control. *Autonomous Robots*,  
573    13, 21–35.
- 574    Bak, T., & Jakobsen, H. (2004). Agricultural Robotic Platform with Four  
575    Wheel Steering for Weed Detection. *o*, 87, 125–136.
- 576    Barawid, O. C., Mizushima, A., Ishii, K., & Noguchi, N. (2007). Devel-  
577    opment of an Autonomous Navigation System using a Two-dimensional  
578    Laser Scanner in an Orchard Application. *Biosystems Engineering*, 96,  
579    139–149.
- 580    Bawden, O., Kulk, J., Russell, R., Mccool, C., English, A., Dayoub, F.,  
581    Lehnert, C., & Perez, T. (2017). Robot for weed species plant-specific  
582    management. *Journal of Field Robotics*, (pp. 1–21).

- 583 Bell, J., MacDonald, B. A., & Ahn, H. S. (2016). Row following in per-  
584 gola structured orchards. In *2016 IEEE/RSJ International Conference on*  
585 *Intelligent Robots and Systems (IROS)* (pp. 640–645).
- 586 Bergerman, B. M., Maeta, S. M., & Zhang, J. (2015). Robot Farmers.  
587 *Robotics & Automation Magazine*, 1.
- 588 Blackmore, B. S., Griepentrog, H. W., Fountas, S., & Gemtos, T. A. (2007).  
589 A Specification for an Autonomous Crop Production Mechanization Sys-  
590 tem. *Agricultural Engineering International*, IX, 1–24.
- 591 Durrant-Whyte, H. (2005). Autonomous land vehicles. *Proceedings of the In-*  
592 *stitution of Mechanical Engineers, Part I: Journal of Systems and Control*  
593 *Engineering*, 219, 77–98.
- 594 Freitas, G., Hamner, B., Bergerman, M., & Singh, S. (2012). A practical  
595 obstacle detection system for autonomous orchard vehicles. *IEEE Inter-*  
596 *national Conference on Intelligent Robots and Systems*, (pp. 3391–3398).
- 597 Gerkey, B. (2010). gmapping. <http://wiki.ros.org/gmapping>.
- 598 Grisetti, G., Stachniss, C., & Burgard, W. (2007). Improved Techniques for  
599 Grid Mapping With Rao-Blackwellized Particle Filters. *IEEE Transactions*  
600 *on Robotics*, 23, 34–46.
- 601 Hansen, S., Bayramoglu, E., Andersen, J. C., Ravn, O., Andersen, N., &  
602 Poulsen, N. K. (2011). Orchard navigation using derivative free Kalman  
603 filtering. *Proceedings of the 2011 American Control Conference*, (pp. 4679–  
604 4684).
- 605 He, B., Liu, G., Ji, Y., Si, Y., & Gao, R. (2011). Auto recognition of navi-  
606 gation path for harvest robot based on machine vision. *IFIP Advances in*  
607 *Information and Communication Technology*, 344 AICT, 138–148.
- 608 Klose, R., Thiel, M., Ruckelshausen, a., & Marquering, J. (2008). Weedy  
609 – a sensor fusion based autonomous field robot for selective weed control.  
610 *Land. Technik 2008*, 2045, 167–172.
- 611 LeCun, Y., Bengio, Y., & Hinton, G. (2015). Deep learning. *Nature*, 521,  
612 436–444.

- 613 Li, M., Imou, K., Wakabayashi, K., & Yokoyama, S. (2009). Review of re-  
614 search on agricultural vehicle autonomous guidance. *International Journal*  
615 *of Agricultural and Biological Engineering*, 2, 1–16.
- 616 Long, J., Shelhamer, E., & Darrell, T. (2015). Fully convolutional networks  
617 for semantic segmentation. In *Proceedings of the IEEE Conference on*  
618 *Computer Vision and Pattern Recognition* (pp. 3431–3440).
- 619 Pedersen, S. M., Fountas, S., Have, H., & Blackmore, B. S. (2006). Agricultural  
620 robots - System analysis and economic feasibility. *Precision Agriculture*,  
621 7, 295–308.
- 622 Pedersen, T. S., Nielsen, K. M., Andersen, P., & Nielsen, J. D. (2002). Develop-  
623 opment of an Autonomous Vehicle for Weed and Crop Registration. *Inter-*  
624 *national Conference on Agricultural Engineering AgEng2002, Budapest,*
- 625 Ruckelshausen, A., Biber, P., Dorna, M., Gremmes, H., Klose, R., Linz,  
626 A., Rahe, F., Resch, R., Thiel, M., Trautz, D., Weiss, U., Doma, M., &  
627 Rahne, R. (2009). BoniRob: an autonomous field robot platform for indi-  
628 vidual plant phenotyping. *Proceedings of Joint International Agricultural*  
629 *Conference (2009)*, 9, 841–847.
- 630 Scarfe, A. J. (2012). *Development of an Autonomous Kiwifruit Harvester.*  
631 (unpublished doctoral dissertation). Massey University, Palmerston North,  
632 New Zealand.
- 633 Scarfe, A. J., Flemmer, R. C., Bakker, H. H., & Flemmer, C. L. (2009).  
634 Development of an autonomous kiwifruit picking robot. In *Autonomous*  
635 *Robots and Agents, 2009. ICARA 2009. 4th International Conference on*  
636 (pp. 380–384). IEEE.
- 637 Seabright, M., Barnett, J., Jones, M. H., Martinsen, P., Schaare, P., Bell,  
638 J., Williams, H., Nejati, M., Seok, H. A., Lim, J., Scarfe, A., Duke, M.,  
639 & MacDonald, B. (2017). Automated Pollination of Kiwifruit Flowers. In  
640 *7th Asian-Australasian Conference on Precision Agriculture (7ACPA)*.
- 641 Sharifi, M., & Chen, X. (2015). A novel vision based row guidance approach  
642 for navigation of agricultural mobile robots in orchards. *ICARA 2015*  
643 - *Proceedings of the 2015 6th International Conference on Automation,*  
644 *Robotics and Applications*, (pp. 251–255).

- 645 Slaughter, D. C., Giles, D. K., & Downey, D. (2008). Autonomous robotic  
646 weed control systems: A review. *Computers and Electronics in Agriculture*,  
647 61, 63–78.
- 648 Statistics New Zealand (2015). Annual Fruit Exports Hit \$2 Billion for First  
649 Time.
- 650 Subramanian, V., Burks, T. F., & Arroyo, A. A. (2006). Development of  
651 machine vision and laser radar based autonomous vehicle guidance systems  
652 for citrus grove navigation. *Computers and Electronics in Agriculture*, 53,  
653 130–143.
- 654 Timmins, J. (2009). Seasonal Employment Patterns in the Horticultural  
655 Industry.
- 656 Torres-Sospedra, J., & Nebot, P. (2011). A New Approach to Visual-Based  
657 Sensory System for Navigation into Orange Groves. *Sensors*, 11, 4086–  
658 4103.
- 659 Williams, H., Jones, M. H., Nejati, M., Bell, J., Penhall, N., Seok, H. A.,  
660 Lim, J., MacDonald, B., Seabright, M., Barnett, J., Duke, M., & Scarfe, A.  
661 (2018). Robotic Kiwifruit Harvesting using Machine Vision, Convolutional  
662 Neural Networks, and Robotic Arms. *Biosystems Engineering*, (p. To be  
663 published).
- 664 Zhang, J., Maeta, S., Bergerman, M., & Singh, S. (2014). Mapping Orchards  
665 for Autonomous Navigation. *ASABE Annual International Meeting*, 7004,  
666 1–9.